Vol. 35, No. 3 (2013) 177-189

Tribology in Industry

www.tribology.fink.rs

RESEARCH

A Comparison of Porous Structures on the Performance of a Magnetic Fluid Based Rough Short Bearing

J.R. Patel[a], G.M. Deheri[a]

[a]*Department of Mathematics, Sardar Patel University, V.V. Nagar, Anand, Gujarat, India.*

Keywords:

Short Bearing
Magnetic Fluid
Rough Surfaces
Load Carrying Capacity
Porosity

Corresponding author:

Jimit R. Patel
[a]*Department of Mathematics,*
Sardar Patel University,
V.V. Nagar,
Anand,
Gujarat,
India.
E-mail:
patel.jimitphdmarch2013@gmail.com

A B S T R A C T

Efforts have been made to study and analyze the comparison of various porous structures on the performance of a magnetic fluid based transversely rough short bearing. The globular sphere model of Kozeny-Carman and Irmay's capillary fissures model have been subjected to investigations. The transverse surface roughness of the bearing surfaces has been characterized by a stochastic random variable with non zero mean, variance and skewness. The stochastically averaged Reynolds type equation has been solved under suitable boundary conditions to obtain the pressure distribution in turn which gives the expression for the load carrying capacity. It is found that the magnetization affects the bearing system positively while the bearing suffers owing to transverse roughness. This adverse effect is relatively less in the case of Kozeny-Carman model. The negatively skewed roughness induces an increase in load carrying capacity which can be channelized to compensate the adverse effect of porosity, at least in the case of Kozeny-Carman model. This compensation in the case of Irmay's model is relatively less. The effect of magnetization responds more in the case of Kozeny-Carman model as compared to Irmay's model.

1. INTRODUCTION

Lubricated bearings are well known in industrial applications and their main advantages compared with rolling and friction bearings are their law friction and very high precision. The biomedical application and the investigation of the reheological properties of magnetic fluids gained considerable importance during the last years. In fact, investigations of the properties, the flow and the application possibilities of suspensions of magnetic nano particles are an extremely lively research field nowadays. Recent experimental as well as theoretical investigations have established that the formation of structure of magnetic nano particles has significant influence on the magneto viscous behavior of ferrofluids.

Nada and Osman [1] investigated the problem of lubrication of finite hydrodynamic journal bearing lubricated by magnetic fluids with couple stress, based upon the Stokes micro-continnum theory. It was established that the bearing characteristics enhanced due to the magnetic effects Fe_30_4 based ferrofluids with different saturation magnetization were employed by Huang et al. [2] to study the supporting capacity and tribological performance of ferrofluids. Urreta et al. [3] summarized the work carried out in the domain of hydrodynamic lubricated journal bearings with magnetic fluids. Here, it was mooted that magnetic fluids could be used to develop active journal bearings. By applying an external magnetic field, ferrofluids can be confined, positioned, shaped and controlled at a desire location. Huang et al. [4] conducted a discussion on the ferrofluid lubrication with an external magnetic field and found that the load carrying capacity of a lubricant film of a magnetic fluid increased with an appropriate magnetic field.

On the basis of Stokes theory and Christensen stochastic model, Chiang et al. [5] theoretically studied the combined effect of couple stresses and surface roughness on the instability thresholds of a rough short journal bearing lubricated with non-Newtonian fluids. Here the couple stress accompanied with longitudinal roughness to provide an increase in the stability threshold speed. Deresse and Sinha [6] analyzed the roughness and thermal effect on different characteristics of finite rough tilted pad slider bearings. It was observed that for non-parallel slider bearings the load carrying capacity due to combined effect was less than the load capacity due to roughness effect for both longitudinal and transverse roughness model. Nuduvinamani et al. [7] launched a theoretical analysis of the problem of magneto hydrodynamic couple stress fluid film lubrication between rough circular stepped plats. It was found that the radial roughness patterns on the bearing surface decreased the mean load capacity and squeeze film time. Further, the applied magnetic field increased the load carrying capacity. Adamu and Sinha [8] discussed the roughness and thermal effects on the performance characteristics of an infinitely long tilted pad slider bearing considering heat conductivity through both the pad and slider. Vakis and Polycarpou [9] proposed a model to study the mixed nano lubrication regime expected during light contact or “surfing”, recording in magnetic storage. In fact they presented an advanced rough surface continuum based contact and sliding model in the presence of molecularly thin lubricant. Zhu and Wang [10] studied the effect of roughness orientation on the elastrohydrodinamic lubrication film thickness. The orientation effect for circular or elliptical contact problems appeared to be more complicated than that for line contacts due to the existence of significant lateral flows. The longitudinal roughness here was more favorable.

Tzeng and Seibel [11] recognized the random nature of roughness orientation and used a stochastic method to describe the surface roughness. Later on, this was developed by Christensen and Tonder [12-14] to propose a more general method for analyzing the effect of both the roughness patterns (transverse as well as longitudinal). This method was employed by Gupta and Deheri [15] to conduct an analysis for the performance of a rough spherical bearing.

Elsharkawy and Nassar [16] dealt with the hydrodynamic lubrication of squeeze film porous bearings. The load carrying capacity decreased with the increase in permeability parameter. The effect of porous layer on the hydrodynamic lubrication of squeeze film porous bearing could be neglected when the permeability parameter was less than 0.001. Elsharkawy and Alyaqout [17] considered the optimum shape design for the surface of a porous slider bearing lubricated with a couple stress fluids. The results established that the optimization approach reduced the coefficient of friction. In addition, the slip parameter significantly affected the optimum friction.

Deheri and Patel [18] discussed the transverse roughness effect on the performance characteristics of a magnetic fluid based short bearing. Here it was shown that the effect of transverse roughness remained always adverse irrespective of the strength of the magnetic field. However, this situation was a little better when negatively skewed roughness pattern occurred. Patel et al. [19] considered the performance of a hydrodynamic short journal bearing under the presence of a magnetic fluid lubricant. It was shown that the magnetization turned in a favorable effect on the performance of the bearing system. The coefficient of friction decreased significantly for a large range of the magnetization parameter. Recently, Shimpi and Deheri [20] considered the effect of roughness and deformation on the configuration of the problem effect on short bearing studied by Deheri and Patel [18]. This article suggested that the negative of the standard deviation associated with the roughness could be neutralized up to certain extent by the positive effect of the magnetization parameter, by suitably choosing film thickness ratio, when the deformation was comparatively less.

Patel et al. [21] considered the magnetic fluid lubrication of a squeeze film between transversely rough triangular plates. Here, it was shown that the magnetic field induced positive effects reduced the adverse effect of transverse roughness to certain extent when negative variance was involved. Singh et al. [22] investigated the effect of non Newtonian lubricant blended with viscosity index improver on the performance of a pivoted curved slider bearing considering Rabinowitsch fluid model. Myshkin and Grigoriev [23] reviewed the main methods of surface roughness analysis. Advantages and disadvantages of traditional and modern approaches of surface analysis based on concepts of roughness and texture were discussed.

Here, it has been carry out to a comparative study of different porous structures on the performance of a magnetic fluid based transversely rough short bearing.

2. ANALYSIS

The geometry and configuration of the present bearing system is shown in the Fig.1. The slider moves with the uniform velocity u in the X-direction.

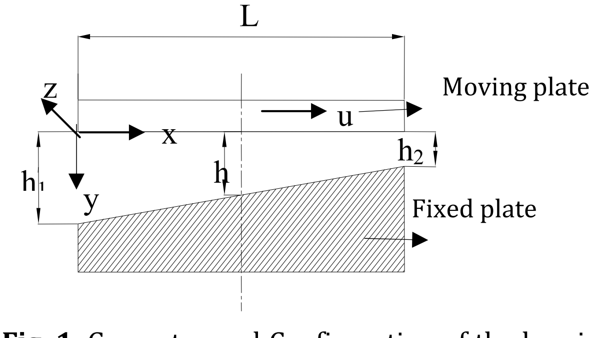

Fig. 1. Geometry and Configuration of the bearing system**.**

The length of the bearing is L and breadth B is in Z-direction where B<<L, necessitating dimension of B to be very small. The pressure gradient $\partial p/\partial Z$, is much larger as compared to the pressure gradient $\partial p/\partial X$ and hence the latter can be neglected.

It is assumed that the bearing surfaces are transversely rough. In line with the discussions of Christensen and Tonder [12-14], the thickness $\mathrm{h(x)}$ of the lubricant film is taken as:

$$\mathrm{h}(\mathrm{x}) = \bar{\mathrm{h}}(x) + h_s$$

where $\bar{\mathrm{h}}(x)$ is the mean film thickness and h_s is the deviation from the mean film thickness characterizing the random roughness of the bearing surfaces. h_s is considered to be stochastic in nature and governed by the probability density function:

$$f(h_s) = \begin{cases} \dfrac{35}{32c}\left(1-\dfrac{h_2^2}{c^2}\right)^3, -c \le h_s \le c \\ 0, elsewhere \end{cases}$$

wherein c is the maximum deviation from the mean film thickness. The mean α, the standard deviation σ and the parameter ε which is the measure of symmetry of the random variable h_s are defined and discussed in Christensen and Tonder [12-14].

It is taken into account that the lubricant film is isoviscous and incompressible and the flow is laminar. Following, Agrawal [24] the magnetic field is considered to be oblique to the stator. Prajapati [25] carried out the investigation of the effect of various forms of magnitude of the magnetic field. Following his emphasis on certain forms of the magnitude in this study, the magnitude of the magnetic field is taken as:

$$M^2 = KB^2\left\{\left(\frac{1}{2}+\frac{z}{B}\right)\sin\left(\frac{1}{2}-\frac{z}{B}\right)+\left(\frac{1}{2}-\frac{z}{B}\right)\sin\left(\frac{1}{2}+\frac{z}{B}\right)\right\}$$

where K is a suitably chosen constant from dimensionless point of view (Bhat and Deheri [26]).

Under the usual assumptions of hydro magnetic lubrication (Bhat [27]; Prajapati [25]; Deheri, et. al. [28]) the Reynolds equation governing the pressure distribution is obtained as:

$$\frac{d^2}{dz^2}\left(p-\frac{\mu_0\bar{\mu}M^2}{2}\right)=\frac{6\mu u}{g(h)}\frac{dh}{dx} \qquad (1)$$

where:

$$g(h)=h^3+3h^2\alpha+3\left(\sigma^2+\alpha^2\right)h+3\sigma^2\alpha+\alpha^3+\varepsilon+12\psi l_1$$

while μ_0 is the magnetic susceptibility, $\bar{\mu}$ is the free space permeability, μ is the lubricant viscosity and ψ is permeability of porous region.

The concerned boundary conditions are:

$$p=0; z=\pm\frac{B}{2}$$

and

$$\frac{dp}{dz}=0; z=0 \qquad (2)$$

Case-1: (A globular sphere model)

A porous material is filled with globular particles (a mean particle size D_c) which is given in Figure A.

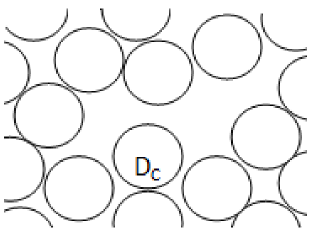

Fig. A. Structure model of porous sheets given by Kozeny-Carman.

The Kozeny-Carman equation is a well-known relation used in the field of fluid dynamics to calculate the pressure drop of a fluid flowing thought a packed bed of solids. This equation remains valid only for laminar flow. The Kozeny-Carman equation mimics some experimental trends and hence serves as a quality control tool for physical and digital experimental results. The Kozeny-Carman equation is very often presented as permeability versus porosity, pore size and turtuosity.

The pressure gradient is assumed to be linear. In view of the discussion Liu [29] the use of Kozeny-Carman formula leads to:

$$\psi=\frac{D_c^2e^3}{72(1-e)^2}\frac{l}{l'}$$

where e is the porosity and $\frac{l'}{l}$ is the length ratio. Under suitable assumptions this ratio turns out to be around 2.5 from experimental results. In that case the Kozeny-Carman formula becomes:

$$\psi=\frac{D_c^2e^3}{180(1-e)^2}.$$

Introducing the dimensionless quantities:

$$m=\frac{h_1-h_2}{h_2}, h=h_2\left\{1+m\left(1-\frac{x}{L}\right)\right\}, l^*=\frac{l}{l'}$$

$$P=\frac{h_2^3}{\mu uB^2}p, \mu^*=\frac{h_2^3k\mu_0\bar{\mu}}{\mu u}, Z=\frac{z}{B}, X=\frac{x}{L},$$

$$A=\{1+m(1-X)\}$$

$$\bar{L}=\frac{L}{h_2}, \bar{\sigma}=\frac{\sigma}{h_2}, \bar{\alpha}=\frac{\alpha}{h_2}, \bar{\varepsilon}=\frac{\varepsilon}{h_2^3}, \bar{\psi}=\frac{D_c^2l_1}{h_2^3} \qquad (3)$$

$$g(\bar{h})=A^3+3A^2\bar{\alpha}+3\left(\bar{\sigma}^2+\bar{\alpha}^2\right)A+3\bar{\sigma}^2\bar{\alpha}+\bar{\alpha}^3+\bar{\varepsilon}+\frac{\bar{\psi}l^*e^3}{6(1-e)^2}$$

and using boundary conditions (2) the dimensionless form of the pressure distribution is found to be:

$$P=\frac{\mu^*}{2}\left\{\left(\frac{1}{2}+Z\right)\sin\left(\frac{1}{2}-Z\right)+\left(\frac{1}{2}-Z\right)\sin\left(\frac{1}{2}+Z\right)\right\}$$
$$+\frac{3m}{\bar{L}}\left(\frac{1}{4}-Z^2\right)\frac{1}{g(\bar{h})} \qquad (4)$$

The load carrying capacity of the bearing system then is obtained as:

$$W=\int_{-B/2}^{B/2}\int_0^L p(x,z)dxdz \qquad (5)$$

Therefore, the non-dimensional load carrying capacity takes the form:

$$W=\frac{h_2^3}{\mu uB^4}w=\mu^*\frac{\bar{L}}{B}(1-\sin(1))+\frac{m}{2}\frac{1}{B}\int_0^1\frac{dx}{g(\bar{h})} \qquad (6)$$

Case-2: (A capillary fissures model)

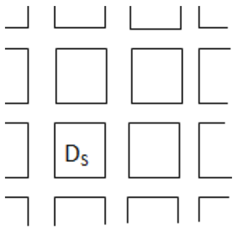

Fig. B. Structure model of porous sheets given by Irmay.

In Figure B, the model consists of three sets of mutually orthogonal fissures (a mean solid size D_s) and assuming no loss of hydraulic gradient at the junctions, Irmay [30] derived the permeability:

$$\psi = \frac{D_s^2\left(1-(1-e)^{2/3}\right)}{12(1-e)}$$

where e is the porosity.

Considering the non-dimensional quantities:

$$g(h^*) = \bar{A}^3 + 3\bar{A}^2\bar{\alpha} + 3\left(\bar{\sigma}^2 + \bar{\alpha}^2\right)\bar{A} + 3\bar{\sigma}^2\bar{\alpha} + \bar{\alpha}^3 + \bar{\varepsilon} + \frac{\psi^*\left(1-(1-e)^{2/3}\right)}{(1-e)}$$

$$\psi^* = \frac{D_s^2 l_1}{h_2^3}$$

and making use of the boundary conditions (2) the dimensionless pressure distribution assumes the form:

$$P = \frac{\mu^*}{2}\left\{\left(\frac{1}{2}+Z\right)\sin\left(\frac{1}{2}-Z\right) + \left(\frac{1}{2}-Z\right)\sin\left(\frac{1}{2}+Z\right)\right\} + \frac{3m}{\bar{L}}\left(\frac{1}{4}-Z^2\right)\frac{1}{g(h^*)} \qquad (7)$$

In view of Equation (5), the non-dimensional load carrying capacity is calculated as

$$W = \frac{h_2^3}{\mu u B^4}w = \mu^*\frac{\bar{L}}{\bar{B}}\left(1-\sin(1)\right) + \frac{m}{2}\frac{1}{\bar{B}}\int_0^1 \frac{dx}{g(h^*)}. \qquad (8)$$

3. RESULTS AND DISCUSSION

It is clearly seen that the pressure increases by:

$$\frac{\mu^*}{2}\left\{\left(\frac{1}{2}+Z\right)\sin\left(\frac{1}{2}-Z\right) + \left(\frac{1}{2}-Z\right)\sin\left(\frac{1}{2}+Z\right)\right\}$$

while the increase in load carrying capacity is:

$$\mu^*\frac{\bar{L}}{\bar{B}}\left(1-\sin(1)\right)$$

as compared to the case of conventional lubricants (for both the models of porosity).

It can be seen from Equation (4, 7) and Equation (6, 8) that the expressions are linear in the magnetization parameter μ^*. Accordingly, the increasing values of μ^* will lead to increased load carrying capacity. Setting the roughness parameters to be zero, this study reduces to the discussion of a magnetic fluid based porous short bearing with different porous structures. Further, considering the magnetization parameter to be zero, this study reduces to the investigation of Basu et al. [31] in the absence of porosity.

The Figs. 2-20 relates to the configuration of Kozeny-Carman (case-1) while the graphical representation for Irmay model (case-2) is presented in Figs. 21-37. The sharp rise in the load carrying capacity is manifest in Figs. 2-3 and Figs. 21-22. This may be probably due to the fact that the magnetization increases the effective viscosity of the lubricant there by increasing the pressure. However Fig. 3 indicates that in the case of Kozeny-Carman model the effect of e on the load carrying capacity with respect to μ^* remains negligible up to the value of $e = 0.15$.

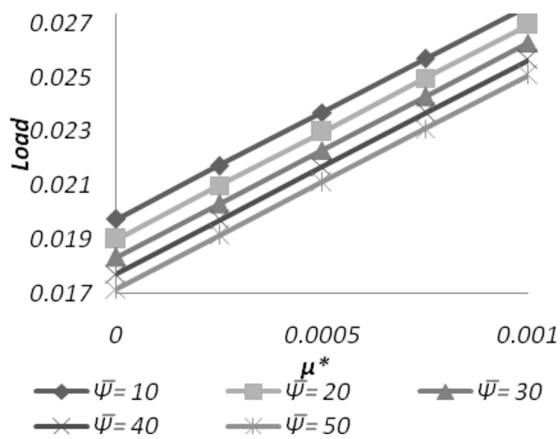

Fig. 2. Variation of load carrying capacity with respect to μ^* and $\bar{\psi}$.

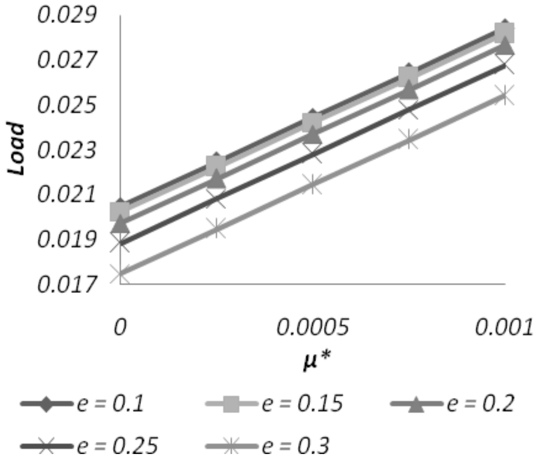

Fig. 3. Variation of load carrying capacity with respect to μ^* and e.

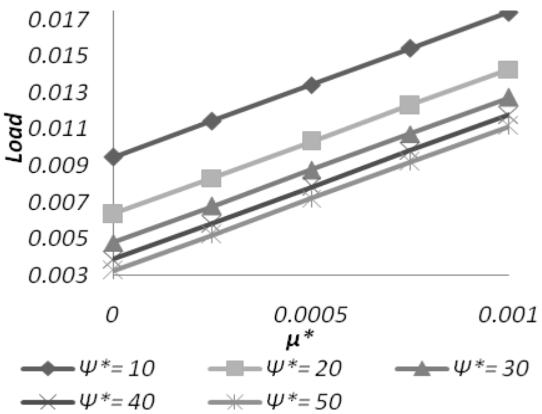

Fig. 21. Variation of load carrying capacity with respect to μ^* and ψ^*.

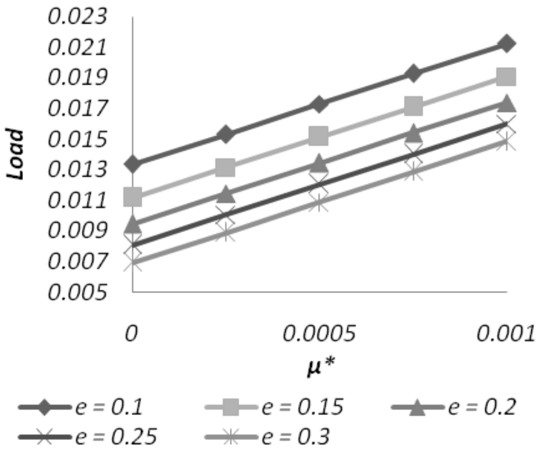

Fig. 22. Variation of load carrying capacity with respect to μ^* and e.

The effect of aspect ratio on the load carrying capacity is presented in Figs. 4-8. It is observed that the aspect ratio causes increased load carrying capacity in the sense that the load carrying capacity increases sharply.

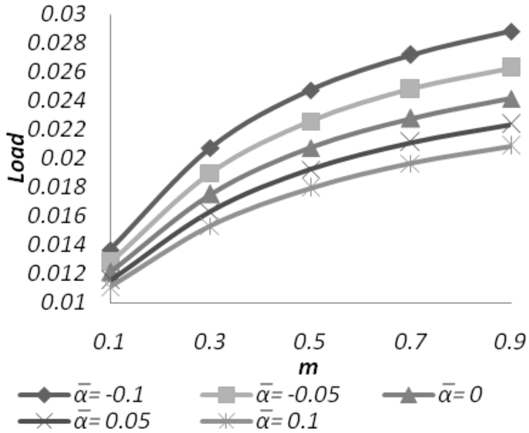

Fig. 4. Variation of load carrying capacity with respect to m and $\bar{\alpha}$.

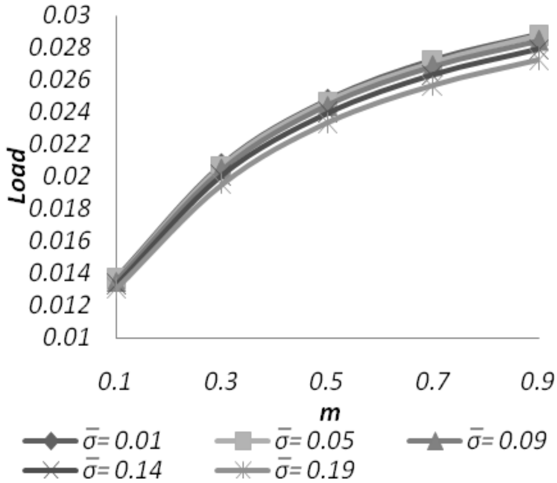

Fig. 5. Variation of load carrying capacity with respect to m and $\bar{\sigma}$.

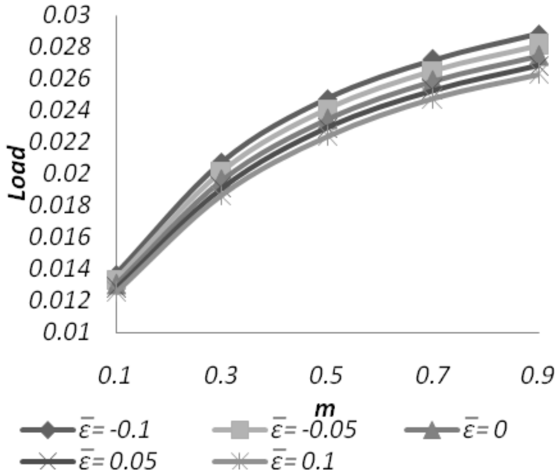

Fig. 6. Variation of load carrying capacity with respect to m and $\bar{\varepsilon}$.

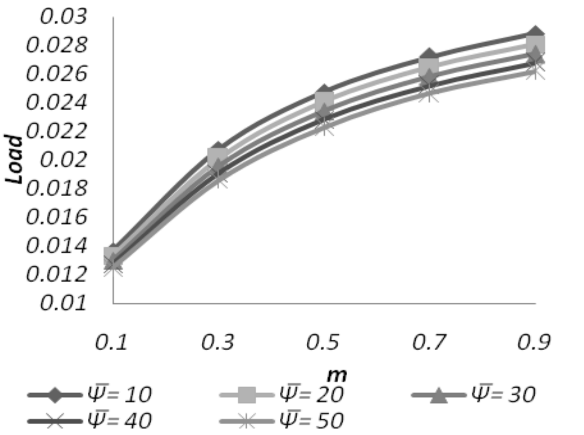

Fig. 7. Variation of load carrying capacity with respect to m and $\overline{\psi}$.

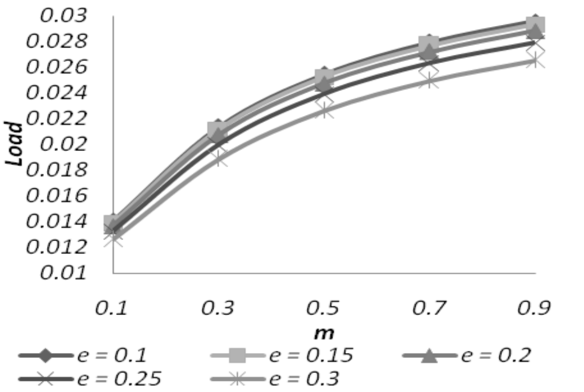

Fig. 8. Variation of load carrying capacity with respect to m and e.

The effect of variance presented in the Figs. 9-12 makes it clear that the load carrying capacity decreases with respect to positive variance while the negative variance induces an increase in the load carrying capacity. Interestingly the effect of standard deviation and e are negligible up to the value of 0.05 as can be seen from Figs. 9 and 12 and 0.15 respectively.

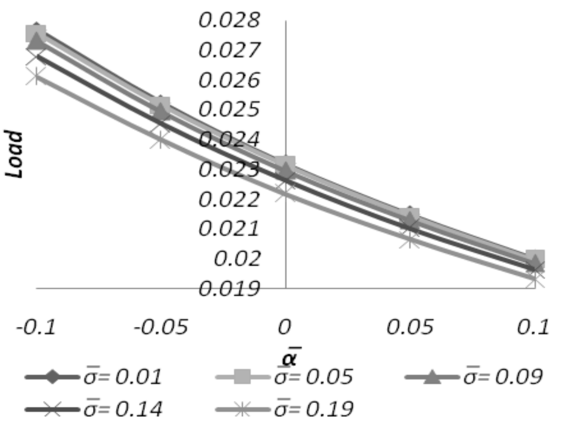

Fig. 9. Variation of load carrying capacity with respect to $\overline{\alpha}$ and $\overline{\sigma}$.

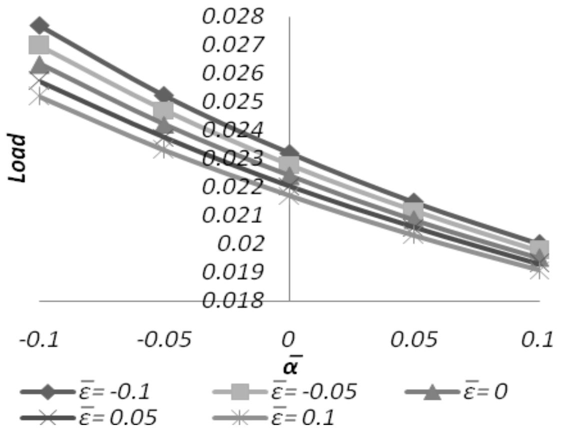

Fig. 10. Variation of load carrying capacity with respect to $\overline{\alpha}$ and $\overline{\varepsilon}$.

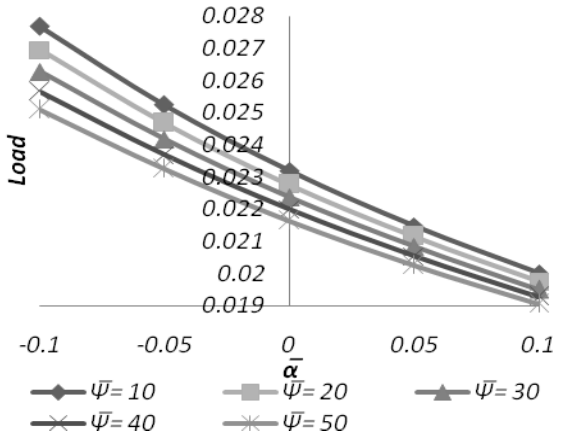

Fig. 11. Variation of load carrying capacity with respect to $\overline{\alpha}$ and $\overline{\psi}$.

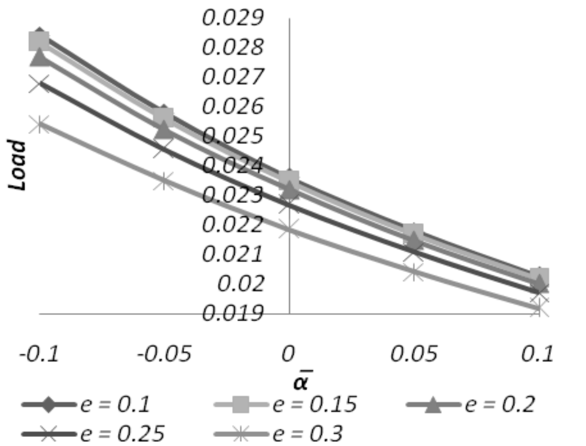

Fig. 12. Variation of load carrying capacity with respect to $\overline{\alpha}$ and e.

The fact that the standard deviation as considerable adverse effect on the performance of the bearing system can be observed from Figs. 13-15 where in the load carrying capacity decreases heavily.

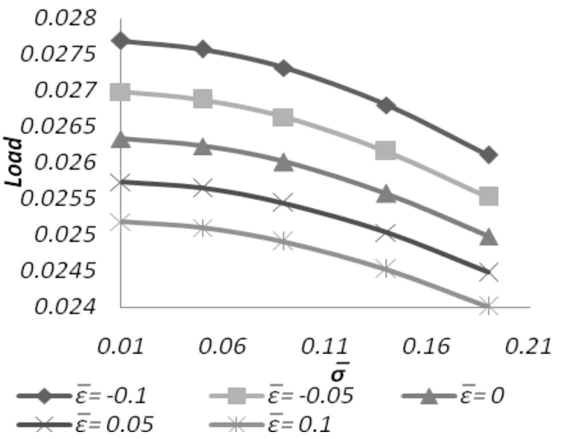

Fig. 13. Variation of load carrying capacity with respect to $\bar{\sigma}$ and $\bar{\varepsilon}$.

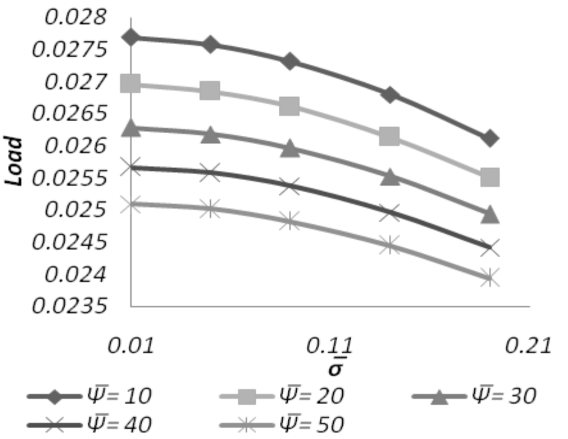

Fig. 14. Variation of load carrying capacity with respect to $\bar{\sigma}$ and $\bar{\psi}$.

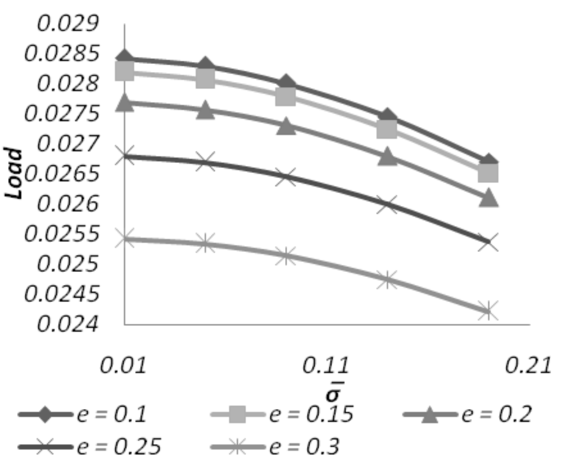

Fig. 15. Variation of load carrying capacity with respect to $\bar{\sigma}$ and e.

The effect of skewness on the load carrying capacity follows the trends of the variance (Figs. 16-17). Therefore the increased load carrying capacity due to variance (negative) gets further increased owing to the negatively skewed roughness.

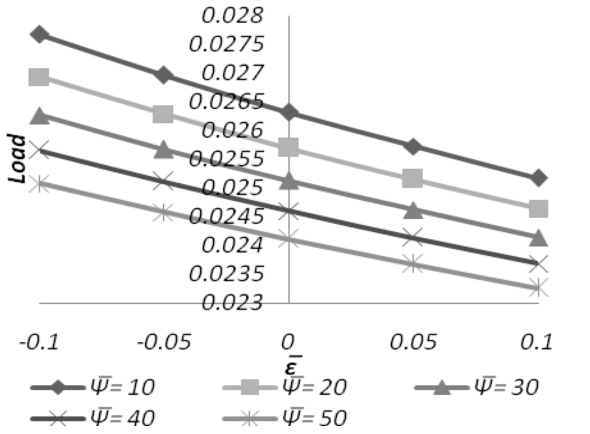

Fig. 16. Variation of load carrying capacity with respect to $\bar{\varepsilon}$ and $\bar{\psi}$.

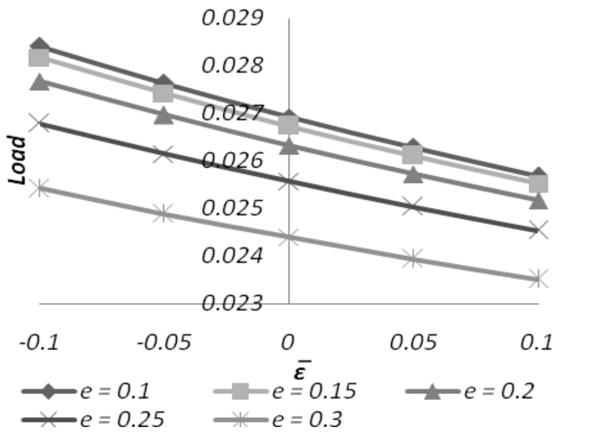

Fig. 17. Variation of load carrying capacity with respect to $\bar{\varepsilon}$ and e.

From Fig. 18 it is noticed that load carrying capacity decreases with increasing values of $\bar{\psi}$. Further the rate of decrease in load carrying capacity with respect to $\bar{\psi}$ gets increased with increasing values of porosity parameter.

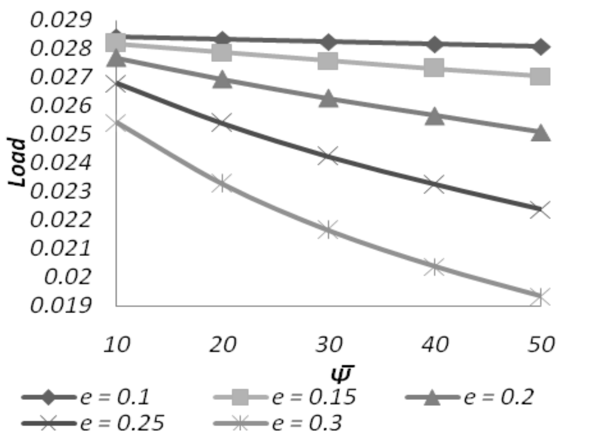

Fig. 18. Variation of load carrying capacity with respect to $\bar{\psi}$ and e.

Figures 19 and 20 bear the testimony of the effect of the ratio l^* on the load carrying capacity. It is clear that the load carrying capacity decreases when l^* increases. The rate of decrease in load carrying capacity due to l^* gets increased with the increasing values of porosity parameter e.

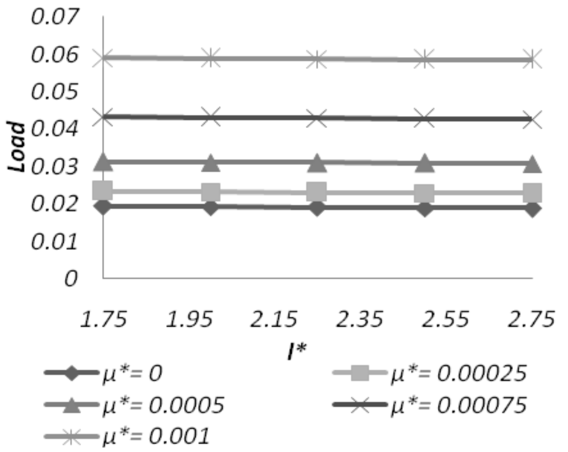

Fig. 19. Variation of load carrying capacity with respect to l^* and μ^*.

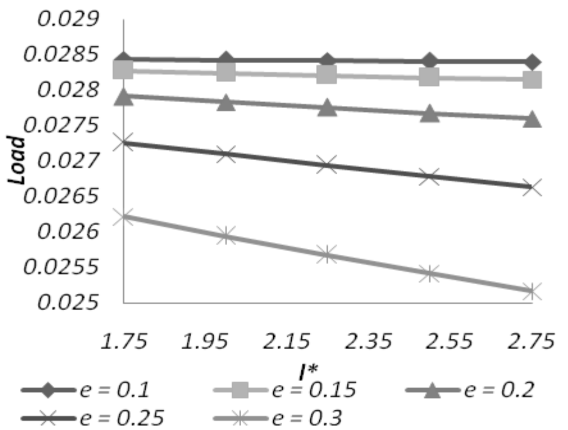

Fig. 20. Variation of load carrying capacity with respect to l^* and e.

The effect of aspect ratio on the load carrying capacity is presented in Figs. 23-27 for Irmay's model. It is clearly observed that the effect of standard deviation on the distribution of load carrying capacity with respect to m is almost negligible. Likewise, the effect of skewness also remains insignificant for a considerable range.

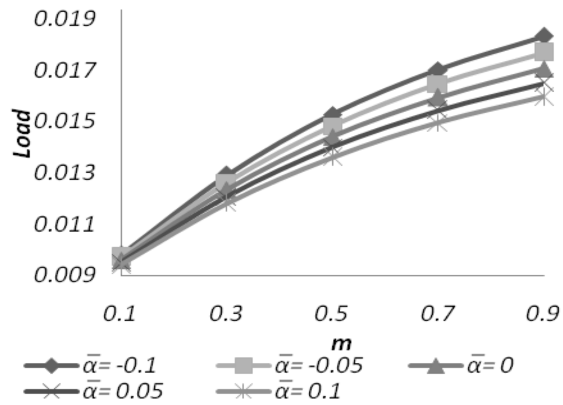

Fig. 23. Variation of load carrying capacity with respect to m and $\bar{\alpha}$.

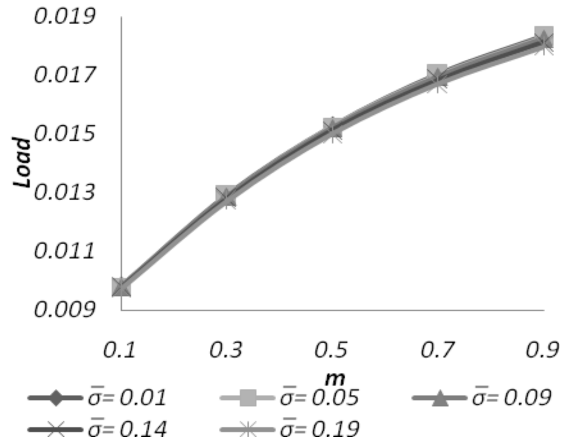

Fig. 24. Variation of load carrying capacity with respect to m and $\bar{\sigma}$.

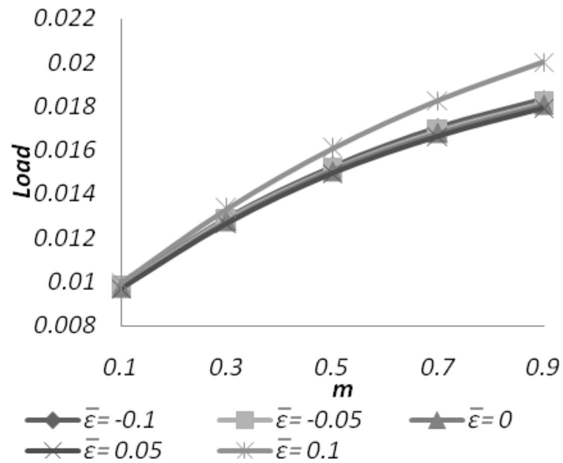

Fig. 25. Variation of load carrying capacity with respect to m and $\bar{\varepsilon}$.

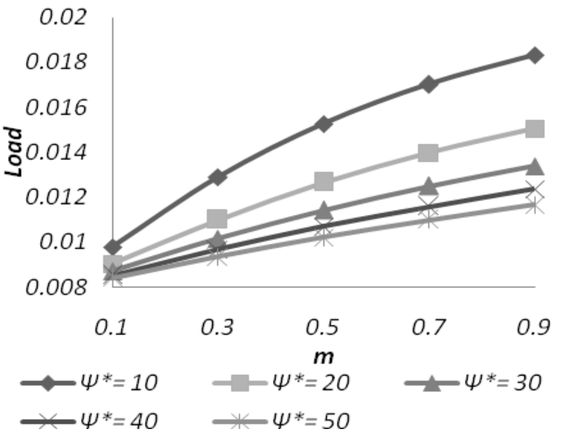

Fig. 26. Variation of load carrying capacity with respect to m and ψ^*.

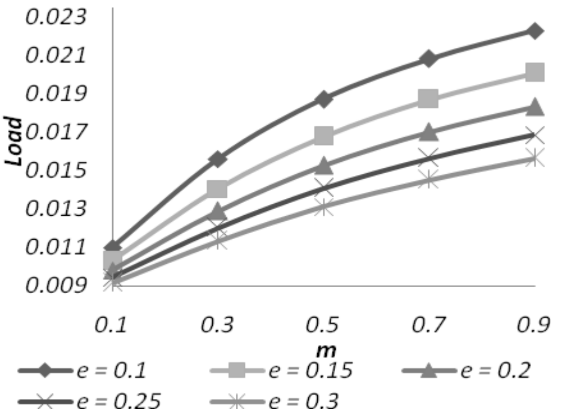

Fig. 27. Variation of load carrying capacity with respect to m and e.

The effect of variance on the load carrying capacity in this case follows the path of the effect of variance on the load carrying capacity in the Kozeny-Carman's case (Figs. 28-31). However, the effect of standard deviation on the distribution of load carrying capacity with respect to variance remains negligible up to the value 0.09.

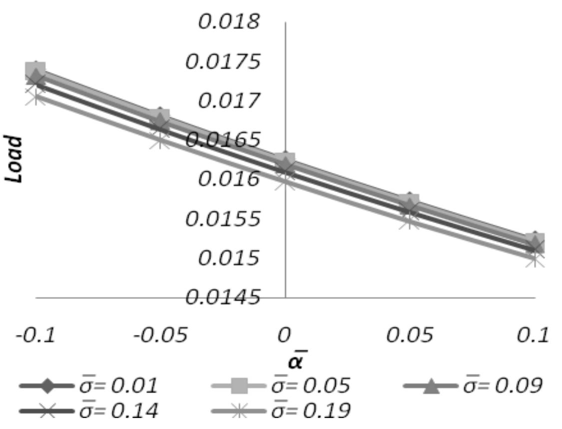

Fig. 28. Variation of load carrying capacity with respect to $\bar{\alpha}$ and $\bar{\sigma}$.

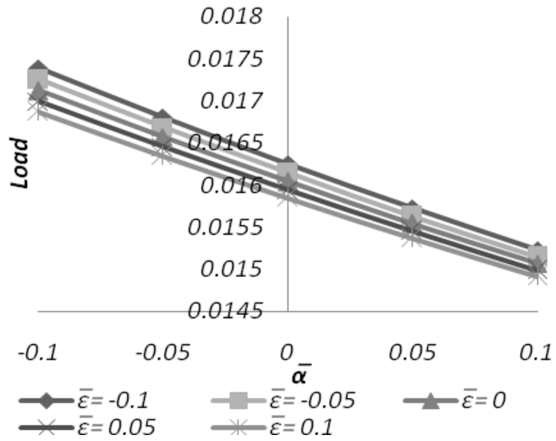

Fig. 29. Variation of load carrying capacity with respect to $\bar{\alpha}$ and $\bar{\varepsilon}$.

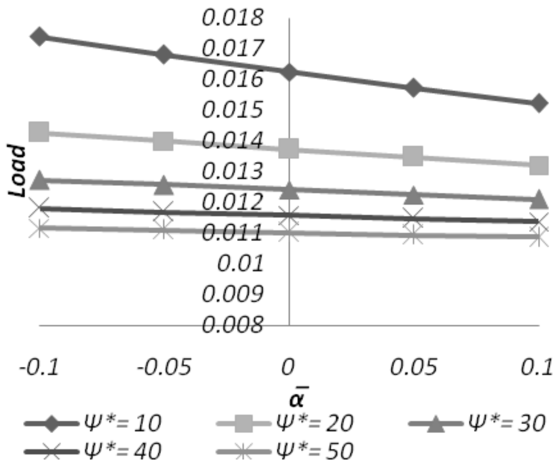

Fig. 30. Variation of load carrying capacity with respect to $\bar{\alpha}$ and ψ^*.

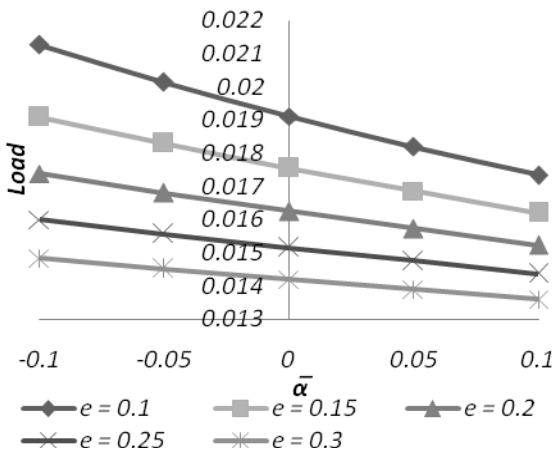

Fig. 31. Variation of load carrying capacity with respect to $\bar{\alpha}$ and e.

The effect of standard deviation on the variation of load carrying capacity is just nominal except in the case of skewness which can be seen from Figs. 32-34.

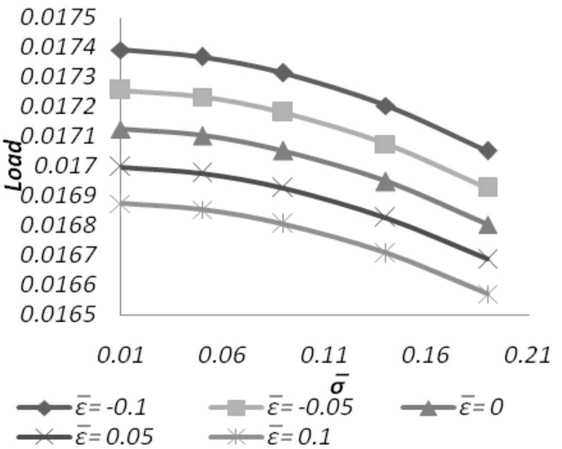

Fig. 32. Variation of load carrying capacity with respect to $\bar{\sigma}$ and $\bar{\varepsilon}$.

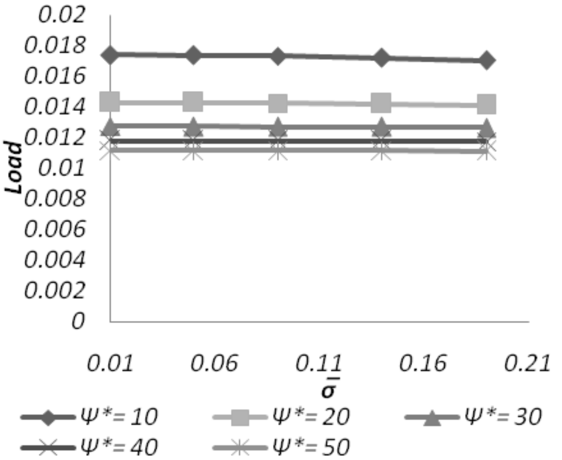

Fig. 33. Variation of load carrying capacity with respect to $\bar{\sigma}$ and ψ^*.

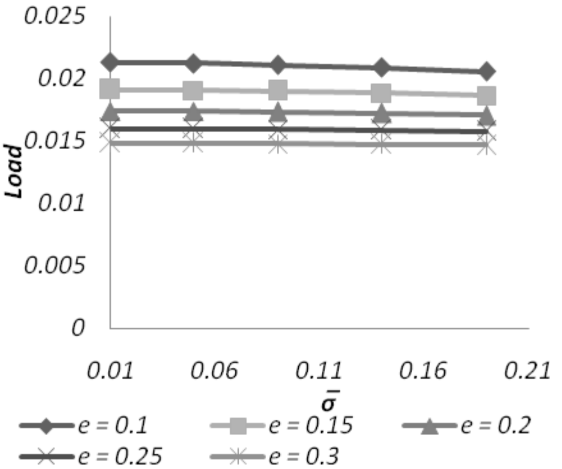

Fig. 34. Variation of load carrying capacity with respect to $\bar{\sigma}$ and e.

The effect of skewness in Figs. 35-36 is not that sharp as compared to the first model, although, it goes along the trends of skewness in the first model.

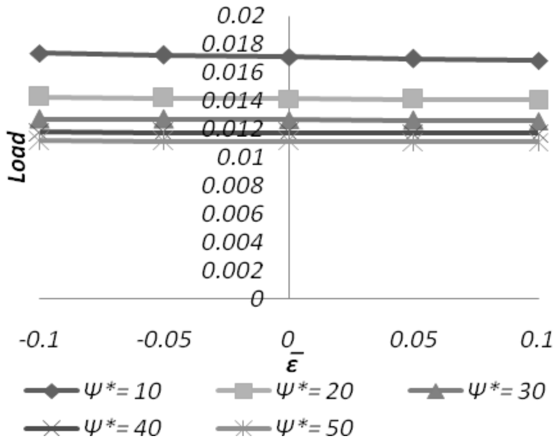

Fig. 35. Variation of load carrying capacity with respect to $\bar{\varepsilon}$ and ψ^*.

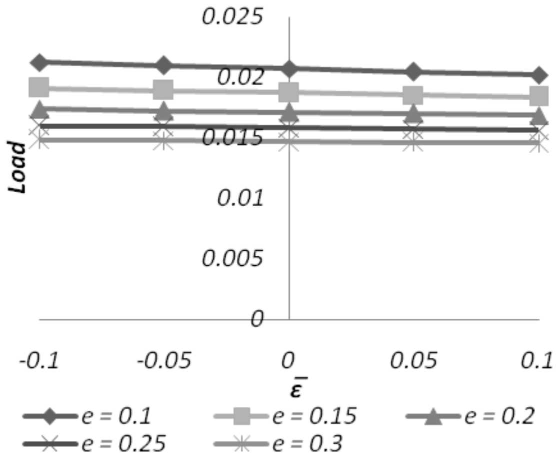

Fig. 36. Variation of load carrying capacity with respect to $\bar{\varepsilon}$ and e.

Lastly, one can easily see from Fig. 37 that the combined effect of ψ^* and e is considerably adverse because the load carrying capacity gets decreased significantly.

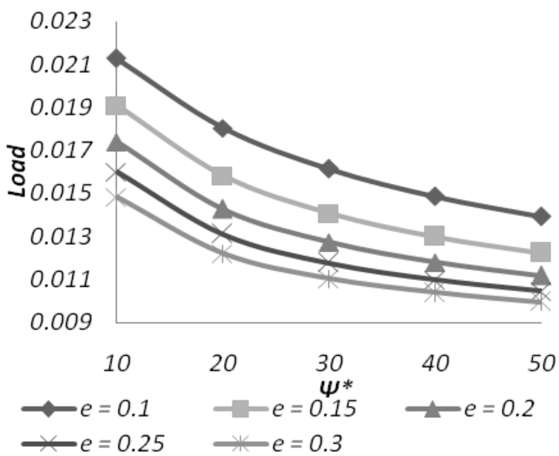

Fig. 37. Variation of load carrying capacity with respect to ψ^* and e.

4. CONCLUSION

First of all this study underlines the importance of the length ratio in the case of Kozeny-Carman. This investigation strongly suggests that the roughness must be duely honoured while designing the bearing system, even if, suitable magnetic strength is in place. A comparison of the results presented here reveals that the Kozeny-Carman model is preferable to gets an overall improved performance. Besides, this article offers an additional degree of freedom from design point of view. Lastly, this type of bearing systems (with the two porous structures) can support certain amount of load even in the absence of flow, which is unlikely, in the case of conventional lubricants.

5. NOMENCLATURE

Symbols		Names
B	=	Width of bearing
h_1	=	Maximum film thickness
h_2	=	Minimum film thickness
μ^*	=	Dimensionless magnetization parameter
$\bar{\sigma}$	=	Dimensionless standard deviation
$\bar{\alpha}$	=	Dimensionless Variance
$\bar{\varepsilon}$	=	Dimensionless Skewness
h	=	Fluid film thickness at any point
L	=	Length of the bearing
m	=	Aspect ratio
M	=	Magnitude of Magnetic field
p	=	Lubricant pressure
P	=	Dimensionless pressure
w	=	Load carrying capacity
W	=	Dimensionless load carrying capacity
α	=	Variance
ε	=	Skewness
σ	=	Standard deviation

Acknowledgements

The authors acknowledge with thanks the comments and suggestions of the reviewers and editor.

REFERENCES

[1] G.S. Nada, T.A. Osman: *Static performance of finite hydrodynamic journal bearings lubricated by magnetic fluids with couple stresses*, Tribol. Lett., Vol. 27, pp. 261-268, 2007.

[2] W. Huang, C. Shen, X. Wang: *Study on static supporting capacity and tribological performance of ferrofluids*, Tribology Transactions, Vol. 52, pp. 717-723, 2009.

[3] H. Urreta, Z. Leicht, A. Sanchez, A. Agirre, P. Kuzhir, G. Magnac: *Hydrodynamic bearing lubricated with magnetic fluids*, Journal of Physics: Conference series, Vol. 149, No. 1, 2009.

[4] W. Huang, C. Shen, S. Liao, X. Wang: *Study on the ferrofluid lubrication with an external magnetic field*, Tribology Lett., Vol. 41, pp. 145-151, 2011.

[5] H.L. Chiang, J.R. Lin, C.H. Hsu, Y.P. Chang: *Linear stability analysis of a rough short journal bearing lubricated with non- Newtonian fluids*, Tribology Lett., Vol. 17, No. 4, pp. 867-877, 2004.

[6] G.A. Deresse, P. Sinha: *THD analysis for finite slider bearing with roughness: special reference to load generation in parallel sliders*, Acta Mech., Vol. 222, pp. 1-15, 2011.

[7] N.B. Naduvinamani, B.N. Hanumegowda, A. Siddanagouda: *Effect of surface roughness on magneto-hydrodynamic couple stress squeeze film lubrication between circular stepped plates*, Lubrication Science, Vol. 24, No. 2, pp. 61-74, 2012.

[8] G. Adamu, P. Sinha: *Thermal and Roughness Effects in a Tilted Pad Slider Bearing Considering Heat Conduction Through the Pad and Slider, Proceedings of the National Academy of Sciences*, India Section A: Physical Sciences, Vol. 82, No. 4, pp. 323-333, 2012.

[9] A.I. Vakis, A.A. Polycarpou: *An Advanced Rough Surface Continuum-Based Contact and Sliding Model in the Presence of Molecularly Thin Lubricant*, Tribology Letters, Vol. 49, No. 1, pp. 227-238, 2013.

[10] D. Zhu , Q.J. Wang: *Effect of Roughness Orientation on the Elastohydrodynamic Lubrication Film Thickness*, J. Tribol., Vol. 135, No. 3, pp. 031501-031509, 2013.

[11] S.T. Tzeng, E. Saibel: *Surface roughness effect on slider bearing lubrication*, Trans. ASLE, Vol. 10, pp. 334-340, 1967.

[12] H. Christensen, K.C. Tonder: *Tribology of rough surfaces: stochastic models of hydrodynamic lubrication*, SINTEF, Report No.10/69-18,1969a.

[13] H. Christensen, K.C. Tonder: *Tribology of rough surfaces: parametric study and comparison of lubrication models*, SINTEF, Report No.22/69-18, 1969b.

[14] H. Christensen, K.C. Tonder: *The hydrodynamic lubrication of rough bearing surfaces of finite width*, in: *Proceedings of the Conference ASME-ASLE Lubrication*, October 12-15, 1970, Cincinnati, OH, pp.12-15.

[15] J.L. Gupta, G.M. Deheri: *Effect of Roughness on the Behavior of Squeeze Film in a Spherical Bearing*, Tribology Transactions, Vol. 39, pp. 99-102, 1996.

[16] A.A. Elsharkawy, M.M. Nassar: *Hydrodynamic lubrication of squeeze-film porous bearings*, Acta Mechanics, Vol. 118, pp. 121-134, 1996.

[17] A.A. Elsharkawy, S.F. Alyaqout: *Optimum shape design for surface of a porous slider bearing lubricated with couple stress fluid*, Lubrication Science, Vol. 21, No. 1, pp. 1–12, 2009.

[18] G.M. Deheri, J.R. Patel: *Effect of surface on the performance of a magnetic fluid based short bearing*, Mathematics Today, Vol. 27, pp. 10-23, 2011.

[19] N.S. Patel, D.P. Vakharia, G.M. Deheri: *A Study on the Performance of a Magnetic-Fluid-Based Hydrodynamic Short Journal Bearing*, ISRN Mechanical Engineering, Vol. 2012, 2012, 7 pages.

[20] M.E. Shimpi, G.M. Deheri: *Effect of deformation in magnetic fluid based transversely rough short bearing*, Tribology - Materials, Surfaces & Interfaces, Vol. 6, No. 1, pp. 20-24, 2012.

[21] R.M. Patel, G.M. Deheri, P.A. Vadher: *Performance of a Magnetic fluid based squeeze film between transversely rough triangular plates*, Tribology in Industry, Vol. 32, No. 1, pp. 33-39, 2010.

[22] U.P. Singh, R.S. Gupta, V.K. Kapur: *On the performance of pivoted curved slider bearings: Rabinowitsch fluid model*, Tribology in Industry, Vol. 34, No. 3, pp. 128-137, 2012.

[23] N.K. Myshkin, A.Ya. Grigoriev: *Roughness and Texture concepts in Tribology*, Tribology in Industry, Vol. 35, No. 2, pp. 97-103, 2013.

[24] V.K. Agrawal: *Magnetic fluid based porous inclined slider bearing*, WEAR, Vol. 107, pp. 133-139, 1986.

[25] B.L. Prajapati: *On Certain Theoretical Studies in Hydrodynamic and Electro-magneto hydrodynamic Lubrication*, Ph.D. Thesis, S.P. University, Vallabh Vidya- Nagar, 1995.

[26] M.V. Bhat, G.M. Deheri: *Porous slider bearing with squeeze film formed by a magnetic fluid*, Pure and Applied Mathematika Sciences, Vol. 39, No. 1-2, pp. 39-43, 1995.

[27] M.V. Bhat: *Lubrication with a Magnetic fluid*, Team Spirit (India) Pvt. Ltd, 2003.

[28] G.M. Deheri, P.I. Andharia, R.M. Patel: *Transversely rough slider bearings with squeeze film formed by a magnetic fluid*, Int. J. of Applied Mechanics and Engineering, Vol. 10, No. 1, pp. 53-76, 2005.

[29] J. Liu: *Analysis of a porous elastic sheet damper with a magnetic fluid*, Journal of Tribology, Vol. 131, pp. 0218011-15, 2009.

[30] S. Irmay: *Flow of liquid through cracked media*, Bull. Res. Counc. Isr., Vol. 5A, No. 1, pp. 84, 1955.

[31] S.K. Basu, S.N. Sengupta, B.B. Ahuja: *Fundamentals of Tribology*, Prentice-Hall of India private limited, New Delhi, 2005.